Understanding the Concept of Basicity in Zeolites. A DFT Study of the Methylation of Al−O−Si Bridging Oxygen Atoms

Pierre Mignon,*,† Paul Geerlings,‡ and Robert Schoonheydt†

Centrum voor Oppervlaktechemie en Katalyse, Kasteelpark Arenberg, 23 B-3001 Heverlee, Belgium, and Eenheid Algemene Chemie (ALGC), Vrije Universiteit Brussel, Pleinlaan 2, 1050 Brussels, Belgium

Received: July 26, 2006; In Final Form: September 15, 2006

DFT calculations on a 4-ring cluster and on ONIOM models of faujasite were carried out to assess the concept of basicity in zeolites, exchanged with alkali cations. The considered reaction is the methylation of the Si−O−Al bridging oxygen by methanol and methyl iodide. The reaction involves both the dissociation of the H_3C-OH or H_3C-I bonds and the formation of the C−O−zeolite bond. The former involves the hardness of the alkaline cation. The latter reflects the charge density of the basic oxygen, well described by the "hard" descriptor: the molecular electrostatic potential. The harder is the alkali metal, the easier is the H_3C-OH or H_3C-I bond dissociation, and the lower is the basicity of the bridging oxygen, and thus the more difficult is the C−O−zeolite bond formation. The fact that these two processes compete has been established by comparing the energy profiles for the methylation with methyl iodide and methanol. For methanol the role of the alkaline metal on the bond dissociation prevails because of the larger hardness of the OH group as compared to that of the iodine atom. For methyl iodide the oxygen basicity prevails over the interaction of I with metal. This study clearly shows that in both experimental and theoretical studies the role of the Lewis acidity or hardness of the alkali metal ion and the role of the basicity of the framework oxygen have to be separated from each other for a good interpretation of zeolite basicity. Also, the hardness of the probe molecule is particularly important when considering the interaction with the alkali metal ion.

Introduction

The interest for basic materials and particularly for basic zeolites considerably increased in the past decade, because of their potential use in catalysis and separation.[1−8] Basic zeolites are most often obtained by exchange with alkaline cations. Conjugate acid−base pairs are then formed. The Lewis acid is the exchangeable metal cation compensating the negative charge of the framework.[9] A framework oxygen, bridging Si and Al and close to the cation, plays the role of basic site.

According to Barthomeuf,[2] basicity is linked to the electron density on the oxygen atom and depends on various factors. It increases with increasing Al content of the framework and with increasing size of the alkaline cation.[9−13] Indeed, in a simplistic view one may say that the more electropositive the compensating cation, the larger the negative charge developed on the structure.[11,14] Hence when considering various alkaline cations the influence of the cation is important. In experimental studies of zeolite basicity, involving adsorbed molecules like CO_2, pyrrole, and NO, it is not often easy to discern the effect of the metal and that of the oxygen atoms from the obtained data.

Pyrrole has been used as a probe molecule to measure the basicity of X and Y zeolites. The N−H group interacts with the framework oxygens and its stretching frequency is taken as a measure of basicity.[15,16] Upon adsorption on LiX and CsX zeolites, the NH stretching band of pyrrole is observed at 3295 and 3175 cm^{-1}, respectively. The lower wavenumber for CsX indicates that the NH group is more strongly bound to the framework oxygen atoms in CsX than in LiX.[17] It is concluded that CsX is more basic than LiX. A XPS study has shown that the bonding energy of the 1s(N) electrons of adsorbed pyrrole is correlated to the size of the alkaline cation and decreases from Li to Cs on X and Y zeolites.[18] The changes in binding energies for the various alkaline metals are attributed to the interaction of the probe molecule with the framework oxygen, but the intrinsic influence of the metal is not discussed. Recently NO^+ was proposed as a new probe molecule for basicity.[19,20] The NO_2 disproportionation produces nitrate and NO^+ ions, the latter being in close interaction with the framework oxygen atoms. The measured frequency of the $\nu(NO^+)$ vibration is believed to be uniquely sensitive to the electron density on the basic oxygen of the zeolite framework. The NO^+ stretching band is observed at 2110 and 1968 cm^{-1} for LiY and RbY, respectively. The frequencies for X zeolites are 15 to 50 cm^{-1} lower indicating a stronger basicity of the oxygen atoms in X. A correlation between $\nu(NO^+)$ and the hardness[21] of the alkaline cation was found for zeolite X. However, for zeolite Y the correlation was weak. Thus, the effect of the metal ion is not clearly evidenced. That of the bridging oxygens of the framework was only indirectly addressed, because the framework was modeled with a set of molecules, covering a basicity range from H_2O to NH_3.

The heterolytic splitting of methyl iodide and methanol in alkaline cation exchanged zeolites gives methoxy groups (reactions 1 and 2),

$$CH_3-OH + M^+-O<Z \leftrightarrow CH_3^+-O<Z + M-OH \quad (1)$$

$$CH_3-I + M^+-O<Z \leftrightarrow CH_3^+-O<Z + M-I \quad (2)$$

* Address correspondence to this author. E-mail: pierre.mignon@biw.kuleuven.be. Phone: +32-16-32-1591.

† Centrum voor Oppervlaktechemie en Katalyse, Kasteelpark Arenberg.

‡ Vrije Universiteit Brussel.

10.1021/jp064762d CCC: $33.50
Published on Web 11/17/2006

which were used as probes of the lattice oxygen basicity.[22−24] It was indeed observed that ^{13}C MAS NMR chemical shift of the methoxy groups linearly depends on the Sanderson electronegativity[25] of the given zeolite structure. The chemisorbed methyl cation does not show any direct interaction with the alkali metal bound to I or OH. Thus the measured signal only depends on the oxygen nucleophilicity. However, reactions 1 and 2 involve both the hardness of the metal for the breaking of the CH_3-OH and CH_3-I bonds and the lattice oxygen basicity for the bonding of the methyl cation to the basic oxygen. Thus, by comparing these two reactions the influence of the alkali cation and of the basicity of the bridging oxygen can be dissociated.

From a theoretical point of view, the concept of basicity in solid materials has been investigated with ab initio techniques and with the electronegativity equalization method (EEM) developed by Mortier.[2,26−29] For a given cation Heidler et al. found that the negative charge on the oxygen of a faujasite model computed from EEM increases when the Si/Al ratio decreases and upon $Na^+ \rightarrow Cs^+$ exchange at constant Si/Al ratio.[9,30] In contrast Deka and co-workers concluded that the net atomic charge computed on the bridging oxygen of a 3T cluster is not a good descriptor of basicity.[31] Instead, soft descriptors such as local softness and relative nucleophilicity[32] were found to correlate with the size of the metal cation. Also a local reactivity descriptor computed from the density of states for an arbitrary bandwidth was found to describe well the basicity for a 6T cluster,[33] even if the smallness of the cluster was criticized for this application.[34] Chamorro and co-workers applied a frontier orbital based approximation for the Fukui function and local softness calculations.[33]

In the present work, soft DFT based descriptors[35] are not considered. Instead we think that hard descriptors such as the molecular electrostatic potential are more reliable to describe the reactivity of a hard center such as a bridging oxygen atom. Also, because the role of the alkali atom is crucial, we study the reaction profiles of the methylation by methyl iodide and methanol (reactions 1 and 2) on a 4T cluster in the gas phase and embedded in a faujasite cluster, encompassing the supercage. As remarked above both the metal ion and the basic oxygen are important for the formation of the surface-bonded methoxy group. Because the hardnesses of hydroxide and iodide ion are quite different, it allows us to gauge the influence of the Lewis acidity/hardness of the alkali metal during the reaction, and thus to gain insight in the role played by the basic oxygen.

Computational Details

The framework of the T4 model was taken from the site III of the X-ray crystal structure of Faujasite.[36] The cluster model was terminated with OH groups and the terminating oxygens were kept fixed during the optimization, only the O−H distances were allowed to vary. The T4 cluster contained one Al and 3 Si atoms and the negative charge is compensated by an alkaline cation. All calculations were performed at the B3LYP/6-31G* level of theory, using the Gaussian 03 suite of programs.[37] SDD basis sets were used for the alkaline metal atoms and for iodine.[38] Previous studies on the application of various DFT functionals for the study of molecular adsorption in zeolite clusters have shown the B3LYP functional to give intermolecular energies and vibrational frequencies close to those obtained at the MP2 level.[39] It was stated that the B3LYP functional was the best choice for DFT treatment of zeolite clusters.[39]

The transition state structures were characterized by means of frequency calculations and analysis of the vibrational modes. It was always checked that only one imaginary frequency was obtained corresponding to the reaction coordinate. Other imaginary frequencies were also obtained, but they correspond to motions of the constrained atoms.

Although these models do not represent accurately the zeolite environment, small clusters have been shown to provide an adequate, qualitative picture of chemical reactions occurring at active sites.[40−42] For example, Rozanska et al.[43] studied the isomerization and transalkylation of toluene and xylenes and found that the relative order of activation energies is conserved when comparing results obtained by using a small T4 cluster and periodic calculations.

Small clusters may correctly represent the active site, but they do not fully incorporate structurally important effects. Larger clusters are needed to capture the pertinent features of the zeolite structure. For this purpose, the ONIOM approach[44] was used, taking into account the whole supercage of faujasite. It subdivides the system into two parts, each described at a different level of theory. The most important one, the *model* system, is described both at the *high* level of theory (B3LYP/6-31G*) and at the *low* level (MNDO), while the entire system, the *real* system, is computed at the *low* level, MNDO. The MNDO level was chosen because it was shown to give good geometries, close to those computed at the HF level, but with cheaper computer resources.[45] The *model* system comprises the same atoms as the cluster model and the *real* system is the supercage of faujasite terminated by hydrogen atoms. The total energy is written as:

$$E^{\mathrm{ONIOM}} = E(\mathrm{high, model}) + E(\mathrm{low, real}) - E(\mathrm{low, model}) \tag{3}$$

During the optimization the influence of the *real* system on the *model* system is passed through the forces, implying that there is no electronic embedding but mechanical embedding. No constraints were imposed and transition states display only one imaginary frequency corresponding to the reaction coordinate. The total number of atoms is 175.

Using the cluster and ONIOM approaches, the reactant, adsorption complex, transition state, and product geometries were optimized for the methylation reaction of the zeolite by both methanol and methyl iodide (see reactions 1 and 2).

Supplementary calculations were performed with ONIOM at a higher level to confirm the results obtained at B3LYP/6-31G*. Optimizations were carried out at B3LYP/6-31+G** and single points at the B3LYP/6-311++G** level. MNDO was used for the *real* system. The notation is B3LYP/6-31+G**/MNDO//B3LYP/6-311++G**/MNDO and the model will be called ONIOM2.

To describe the oxygen basicity we choose hard reactivity descriptors in view of the hard character of the interacting partners and the intrinsic hardness of the oxygen atom. Net atomic charges may be used as an approximation to the local hardness.[46] We thus computed NPA charges. However, atomic charges may behave differently according to the definition of the population analysis used. The molecular electrostatic potential, MEP, gives a more detailed picture of the interaction of the charge density around a given atom with a hard partner (a proton). The MEP at R is given by:

$$V(R) = \sum_A \frac{Z_A}{|R_A - R|} - \int \frac{\rho(r)}{|r - R|}\,\mathrm{d}r \tag{4}$$

where the first summation is overall the nuclei A within the molecule.

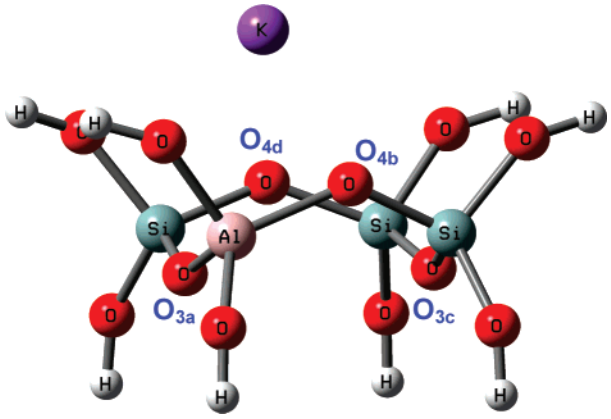

Figure 1. Reactant geometry for the 4T cluster with K^+. The oxygen atoms above the ring are labeled O4 and the oxygen atoms below are labeled O3 in faujasite. The oxygen considered for its basic properties is O4b.

The MEP was computed for the reactants and adsorption complexes. In the reactant complexes the minimum of the MEP around the basic oxygen is computed as a measure of its basicity. This has already been successfully applied in previous works.[47−51] In the adsorption complexes the minimum of the MEP between the basic oxygen and the carbon atom is computed as a measure of the binding affinity between these two atoms.

Results

Geometries. The reactants are the T4 cluster complexed with the alkaline cation, and the isolated methyl iodide or methanol. The T4 cluster is shown in Figure 1 with the charge compensating K^+. The oxygens located at the same side on the 4-ring as the alkaline cation are generally called O_4 in faujasite. The oxygen atoms below the 4-ring are called O_3. The O_4 oxygen atoms have been shown by EEM to be more basic than the O_3 oxygen atoms.[39] In the present study we consider O_{4b} (Al−O−Si bridging oxygen atom) for its basic properties. The adsorption complex is the methanol or methyl iodide adsorbed on the T4 cluster; the transition state describes the methyl cation before chemisorption on the zeolite, while the hydroxyl or iodine is yet not bound to the metal. The product is the hydroxyl or iodide salt and the methylated zeolite (Figure 2).

In the reactant structures of the cluster models (Table 1), the Al−O_{4b} distance (1.80 Å for Li^+) is larger than the value prescribed theoretically (1.74 Å),[2,9] but smaller than the distance observed in acid zeolites (1.89 Å),[52−54] and can thus be attributed to the interaction of the O_{4b} oxygen with the alkali metal. For the ONIOM model, the distances are slightly larger (Table 2), probably because no constraints were imposed during the optimization procedure. Also, the Al−O_{4b} and Si−O_{4b} distances (Tables 1 and 2, cluster and ONIOM models for the reactants structures) increase slightly with decreasing size of the cation, indicating a stronger M−O_{4b} interaction and more ionic bonds for Li^+. Indeed the hard/hard interaction between O_{4b} and the alkali metal ion is expected to be the largest for the hardest metal.

In the adsorption complexes, the bond lengths, C−OH or C−I, do not change with the alkaline cation and they are slightly longer than those of the isolated substituted methanes: 1.41 and 2.19 Å for methanol and methyl iodide, respectively. This is due to the quite strong interaction of the hydroxyl group or iodide with the alkali cation (not yet covalently bound), as can be seen from the small M−OH and M−I distances in Table 1. Also, the C−O_{4b} distance increases with the size of the cation except Li^+. Indeed the larger the cation, the farther it is from the 4-ring and thus the farther are located the substituted methanes from the 4-ring oxygens.

In the transition state structures, we observe the reverse (Tables 1 and 2). The C−O_{4b} distance decreases with increasing size of the cation for the cluster and ONIOM models and both for methanol and methyl iodide. In contrast, the distance C−OH increases with the size of the cation, while the C−I distance is almost constant and independent of the size of the alkaline cation. Thus the interaction of methanol with the alkaline cation is stronger than that of methyl iodide. Indeed, the harder the metal ion is, the stronger the M···OH and M···I interactions and the easier the breaking of the C−OH and C−I bonds, i.e., the breaking of the C−OH and C−I bonds is more difficult in the case of Cs^+ than of Li^+. We notice here that the C−O_{4b} bond formation and the C−OH and C−I bond breaking exhibit opposite trends with respect to the size of the metal cation.

Charges and MEP. The atomic charges can be found in Table 3. The most positive charge on the alkaline metal in the reactant complexes is for Cs^+. The most negative charge on the 4-ring oxygen atoms is observed for Li^+. The average negative charge on the T4 oxygen atoms (AVG) decreases slightly with the size of the alkaline cation. The total average charge over all oxygen atoms of the cluster (Total AVG) is constant and independent of the nature of the alkaline cation. On the basis of the Sanderson's electronegativity principle stating that the more electropositive cation, Cs^+, develops a more intense charge on the zeolite framework, one should have expected a more negatively charged oxygen in the case of Cs^+. On the other hand, these results are not surprising since net atomic charges computed from different schemes of population analysis have already been unsuccessfully tested to describe the oxygen basicity as a function of the type of alkali cation.[31,55,56] Nevertheless, the two oxygen atoms close to the Al atom (O_{4b} and O_{3a}) are more negatively charged than the others and the O_{4b} shows the largest negative charge, which is in agreement with the EEM study.[9] It is also clear from the charges computed for the adsorption complexes and transition states that the most negative charges on O_{4b} are obtained for the smallest/hardest metal. This confirms the failure of atomic charges to describe the oxygen (O_{4b}) basicity.

To evaluate the relative change in basicity of the O_{4b} oxygen for different alkaline metals, we computed the MEP around O_{4b} for the reactants. The data are given in Table 4. One can see for the reactants that the MEP gets more negative when the size of the cation increases. This is confirmed with the calculation of the ONIOM2 model. This means that the oxygen basicity increases from Li^+ to Cs^+, as is expected from experiments. The MEP is then a good choice to describe the reactivity (basicity) of hard centers such as framework oxygen atoms in zeolites. We also computed the minimum of the MEP along the line connecting the oxygen and the carbon atom of the methyl group in the adsorption complexes. The relative trend also follows the same sequence and the facility to form the bond between these two atoms increases with the size of the cation. One can notice that for the reactants and the adsorbed complexes the MEP is deeper for methanol than for methyl iodide.

Energy Profiles. The adsorption energies of methanol and methyl iodide, the activation energies, and the stabilization energies of the products are shown in Table 5, both for the T4 cluster and for the ONIOM models. For methanol and methyl

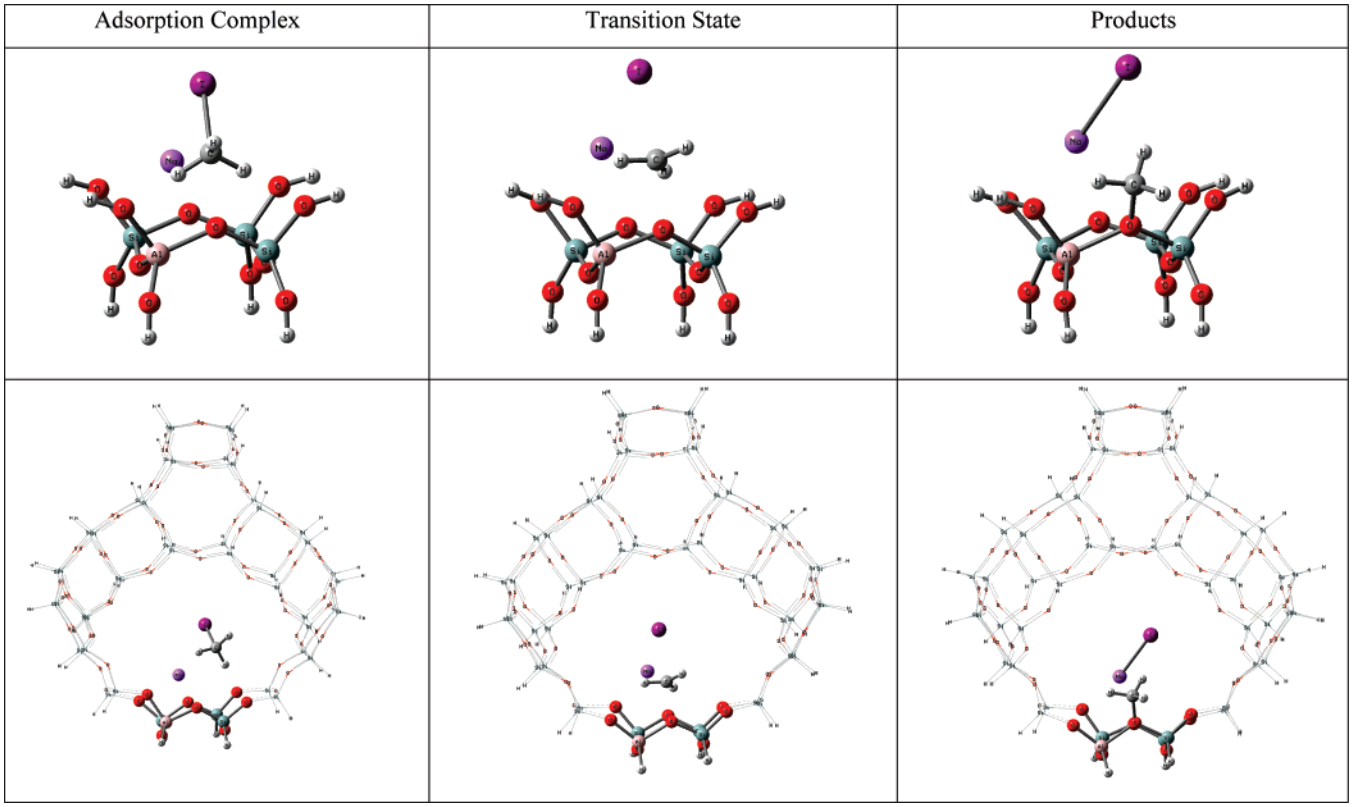

Figure 2. Geometries of the adsorption complex, transition state, and products for the 4T cluster and the ONIOM model, with Na^+.

TABLE 1: Selected Geometrical Parameters for the 4T Cluster (units: Å)

	reactants 4T ring cluster		
	Al−O_{4b}	Si−O_{4b}	M−O_{4b}
Li	1.80	1.63	1.89
Na	1.79	1.63	2.15
K	1.77	1.61	2.64
Rb	1.77	1.60	2.78
Cs	1.76	1.60	2.95

	adsorption complex CH_3OH					adsorption complex CH_3I			
	M−O_{4b}	M−OH	C−OH	C−O_{4b}		M−O_{4b}	M−I	C−I	C−O_{4b}
Li	1.95	1.89	1.45	3.53	Li	1.84	2.89	2.22	4.07
Na	2.39	2.26	1.45	3.29	Na	2.35	3.21	2.22	3.28
K	2.71	2.68	1.44	3.31	K	2.69	3.68	2.22	3.37
Rb	2.83	2.90	1.45	3.37	Rb	2.84	3.88	2.22	3.40
Cs	3.00	3.13	1.44	3.39	Cs	3.01	4.11	2.22	3.41

	transition state CH_3OH					transition state CH_3I			
	M−O_{4b}	M−OH	C−OH	C−O_{4b}		M−O_{4b}	M−I	C−I	C−O_{4b}
Li	4.16	1.74	2.23	1.83	Li	4.38	2.71	2.75	2.06
Na	4.31	2.07	2.31	1.74	Na	4.57	3.00	2.75	2.05
K	4.59	2.40	2.42	1.66	K	4.92	3.44	2.77	2.01
Rb	4.76	2.54	2.51	1.61	Rb	5.01	3.61	2.78	2.00
Cs	4.92	2.68	2.52	1.61	Cs	5.15	3.84	2.80	2.00

iodide the adsorption energies, ΔE_{Ads}, are largest for Li^+. In the case of methanol they decrease with increasing size of the cation both in the T4 and in the ONIOM calculations. For methyl iodide this observation holds for the ONIOM models but not for the T4 cluster. In the latter case there is no clear trend for the adsorption energies of Li^+ and Na^+ over K^+, Rb^+, and Cs^+. This may be due to steric effects (iodide is quite large compared to hydroxyl), to the constraints imposed in the T4 cluster optimization, and to the small size of Li^+ and Na^+ cations. The cluster model seems inadequate to describe the adsorption complex of methyl iodide, while the ONIOM models give a better representation.

The stabilization upon adsorption depends on the interaction of the hydroxyl group or iodide ion with the alkaline metal. The harder the metal, the stronger the M−OH or M−I interaction and, as expected, the stabilization decreases with increasing size of the metal (Table 5). One can notice that the effect of the metal is less important for methyl iodide than for methanol. Iodide is less hard than the oxygen of the hydroxyl, and the M−OH interaction is stronger than the M−I interaction. Thus the adsorption energy mirrors the hardness of the metal.

The activation energies, ΔE_{Act}, for methylation with methanol are comparable to the ones calculated for the reaction of methanol with acid zeolites leading to a methylated zeolite and

TABLE 2: Selected Geometrical Parameters for the ONIOM Model (units: Å)

	reactants 4T ring cluster		
	Al−O4b	Si−O4b	O4b−M
Li	1.87	1.64	1.92
Na	1.81	1.63	2.29
K	1.81	1.62	2.68
Rb	1.80	1.62	2.83

	adsorption complex CH_3OH					adsorption complex CH_3I			
	$M-O_{4b}$	M−OH	C−OH	$C-O_{4b}$		$M-O_{4b}$	M−I	C−I	$C-O_{4b}$
Li	1.92	1.89	1.44	3.67	Li	1.91	2.86	2.22	3.51
Na	2.33	2.25	1.44	3.92	Na	2.33	3.20	2.21	3.73
K	2.72	2.67	1.44	4.09	K	1.73	3.61	2.21	3.86
Rb	2.88	2.86	1.44	3.71	Rb	2.88	3.84	2.20	3.56

	transition state CH_3OH					transition state CH_3I			
	$M-O_{4b}$	M−OH	C−OH	$C-O_{4b}$		$M-O_{4b}$	M−I	C−I	$C-O_{4b}$
Li	4.16	1.75	2.19	1.79	Li	4.37	2.73	2.76	2.02
Na	4.35	2.07	2.25	1.73	Na	4.66	3.00	2.76	2.01
K	4.68	2.41	2.33	1.66	K	2.10	3.43	2.78	1.98
Rb	4.81	2.54	2.35	1.63	Rb	5.23	3.57	2.77	1.97

TABLE 3: NPA Charges Computed for the 4T Cluster with Methanol and Methyl Iodide[a]

	reactants 4T ring cluster					
	O_{4b}	O_{4d}	O_{3c}	O_{3a}	AVG	total AVG
Li	−1.362	−1.282	−1.301	−1.313	−1.315	−1.202
Na	−1.362	−1.287	−1.263	−1.327	−1.310	−1.205
K	−1.335	−1.285	−1.279	−1.318	−1.304	−1.203
Rb	−1.334	−1.286	−1.279	−1.319	−1.305	−1.204
Cs	−1.334	−1.283	−1.278	−1.321	−1.304	−1.204

	adsorption complex CH_3OH					adsorption complex CH_3I			
	O_{4b}	M	C	O		O_{4b}	M	C	I
Li	−1.353	0.872	2.457	−0.829	Li	−1.380	0.863	−0.789	0.034
Na	−1.334	0.907	2.458	−0.814	Na	−1.341	0.894	−0.767	−0.016
K	−1.333	0.943	2.454	−0.800	K	−1.334	0.931	−0.764	−0.036
Rb	−1.335	0.958	2.454	−0.793	Rb	−1.333	0.952	−0.767	−0.043
Cs	−1.332	0.965	2.452	−0.787	Cs	−1.333	0.960	−0.764	−0.040

	transition state CH_3OH					transition state CH_3I			
	O_{4b}	M	C	O		O_{4b}	M	C	I
Li	−1.124	0.589	−0.293	−1.164	Li	−1.176	0.848	−0.417	−0.535
Na	−1.101	0.863	−0.302	−1.152	Na	−1.184	0.894	−0.415	−0.553
K	−1.073	0.679	−0.309	−1.181	K	−1.168	0.937	−0.398	−0.611
Rb	−1.054	0.886	−0.315	−1.190	Rb	−1.172	0.951	−0.393	−0.623
Cs	−1.058	0.911	−0.317	−1.200	Cs	−1.171	0.962	−0.395	−0.625

[a] For the reactants, AVG is the average over O_{4b}, O_{4d}, O_{3c}, and O_{3a}. Total average is the average over all oxygen atoms of the cluster.

TABLE 4: MEP Minima (au) Computed for the 4T Cluster and ONIOM Models with Methanol and Methyl Iodide[a]

	reactants			complex CH_3OH		complex CH_3I	
	4T cluster	ONIOM	ONIOM2	4T cluster	ONIOM	4T cluster	ONIOM
Li	−0.0841	−0.0640	−0.0561	−0.0276	−0.0061	−0.0041	−0.0314
Na	−0.0879	−0.0680	−0.0606	−0.0617	−0.0243	−0.0588	−0.0400
K	−0.0959	−0.0722	−0.0658	−0.0771	−0.0491	−0.0676	−0.0549
Rb	−0.0993	−0.0776	−0.0697	−0.0829	−0.0573	−0.0709	−0.0562
Cs	−0.1043			−0.0869		−0.0776	

[a] In the reactant geometries, "reactants", the values are the minimum around the basic O_{4b} oxygen. ONIOM2 corresponds to the calculations performed at the B3LYP/6-31+G**/MNDO//B3LYP/6-311++G**/MNDO level. In the adsorption complex, "complex", the values are the minimum along the line connecting the carbon of the methyl group and O_{4b}.

a water molecule.[54] There the activation energy is about 53 kcal/mol. This value is quite close to the activation energy for the cluster and ONIOM models with Li^+ (Table 5). One can see that for methanol the activation energy increases with the size of the cation, for both the cluster and the ONIOM models. For methyl iodide in the T4 cluster model the activation energy decreases with increasing size of the cation (except for Na^+). In the ONIOM model this is less clear. For the ONIOM2 model with CH_3I, we observe a clear decrease of the activation energy with the size of the cation. The ONIOM2 model is the more accurate and shows a clear difference between CH_3I and CH_3-OH in the trend of the activation energies. With methyl iodide, the interaction between the soft iodide and the hard metal is weak. In the case of methanol the hard oxygen interacts with

TABLE 5: Energy Profiles (kcal/mol) for the 4T Cluster, ONIOM, and ONIOM2 Models with Methanol and Methyl Iodide.

	cluster			ONIOM			ONIOM2		
	ΔE_{Ads}	ΔE_{Act}	ΔE_S	ΔE_{Ads}	ΔE_{Act}	ΔE_S	ΔE_{Ads}	ΔE_{Act}	ΔE_S
				CH_3OH					
Li	−23.5	54.2	−14.5	−21.6	56.5	−14.2	−39.2	50.6	−14.0
Na	−15.2	62.8	−10.8	−16.3	63.6	−9.9	−33.4	54.7	−9.8
K	−12.5	69.3	−8.7	−12.0	67.6	−5.3	−29.7	56.0	−7.3
Rb	−10.7	70.8	−8.6	−10.0	74.0	−5.4	−28.4	62.5	*b*
Cs	−9.4	73.0	−8.9						
				CH_3I					
Li	−28.5	37.6	−27.4	−6.7	23.0	−21.0	−12.9	22.1	−12.1
Na	−8.1	24.1	−21.8	−5.3	24.6	−19.3	−4.0	16.9	−10.6
K	−10.1	25.5	−27.2	−4.1	22.4	−16.4	−1.3	15.7	−7.6
Rb	−9.9	25.2	−29.2	−2.8	28.0	−24.7	*b*	*b*	−5.9
Cs	−9.7	24.8	−29.7						

[a] ΔE_{Ads} is the difference in energy between the reactants and the adsorption complex. ΔE_{Act} is the difference in energy between the transition state and the Adsorption complex. ΔE_S is the difference in energy between the product and the transition state. [b] Unsuccessful optimization of the products for the complex with methanol and Rb^+. The optimization of the adsorption complex with methyl iodide and Rb^+ leads to unsatisfactory geometries; the methyl iodide was found to be out of the supercage, probably due the large size of Rb^+ and I atoms.

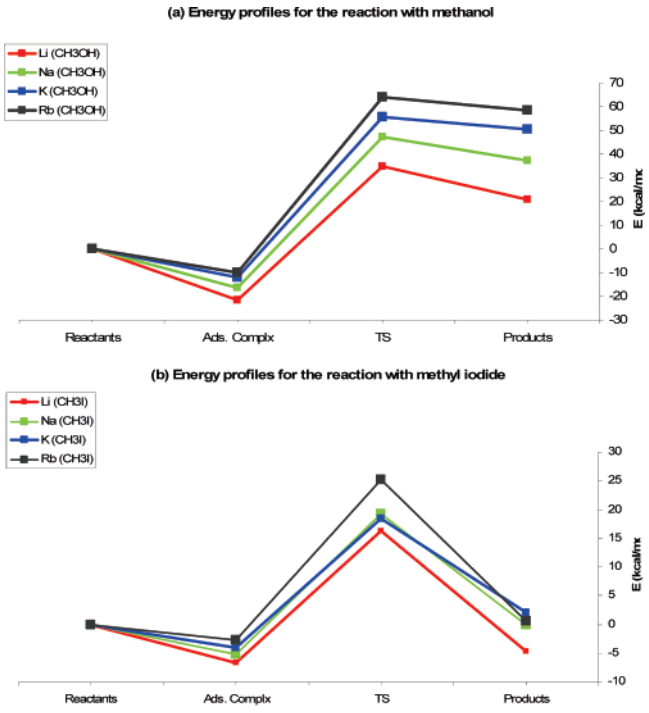

Figure 3. Energy profiles for the ONIOM model computed at the B3LYP/6-31G*/MNDO level. See Table 5.

the hard alkali metal cation. In the latter case the influence of the alkali cation on the activation energies is dominant. For methyl iodide the interaction of O_{4b} and the C of the methyl group is dominant and determines the activation's energy.

The energy profiles of reactions 1 and 2, calculated in the ONIOM model, are shown in Figure 3. We observe that in the case of methanol the reaction is endothermic, whatever the alkali metal. This is also the case for methyl iodide, except for Li^+. In comparison the methylation of an acidic zeolite model was found to be exothermic.[54] We observe that the energy profiles for different metal ions are more clearly distinguishable for methanol than for methyl iodide. That may be explained by the fact that the interactions of the metal ions are stronger with the hydroxyl group than with the iodide ion.

Discussion

In the methylation of the Si−O−Al bridging oxygen atoms of alkaline cation exchanged zeolites with methyl iodide and methanol two parameters come into play. First, the hardness of the metal that interacts directly with I or OH for the breaking of the C−I or C−OH bonds. Second, the basicity of the bridging oxygen for the bond formation with the carbon atom of the methyl group.

The hardness of the metal can be easily computed within the DFT framework.[35] The hardness is known to increase with decreasing size of the atom and increasing charge. The net atomic charges of the alkaline cations (Table 3) increase with the size of the cation. This is opposite to the hardness. The basicity of the bridging oxygen O_{4b} increases with the size of the alkaline cation. This is also not well described by the atomic charges of O_{4b}. The latter become less negative with increasing size of the alkali cation both in the adsorption complexes and in the transition states. The changes are small and can hardly be used to describe basicities. However, the MEP becomes more negative with increasing size of the alkali cations at all levels of calculation. This is in line with experimentally observed basicity trends. The MEP can reliably be used to represent the basicity.

In the methylation reaction two parameters come into play: the metal hardness in the breaking of the C−O and C−I bonds and the oxygen basicity in the formation of the O_{4b}−C bond. Both vary in the opposite way with the nature of the alkali metal. This leads to opposite effects on the methylation reaction. The M···OH/M···I hard−hard interactions become stronger (ΔE_{Ads} becomes more negative) when the size of the metal decreases. Thus bond breaking is "easier" in the presence of Li^+ than of Cs^+. From the computed MEP values we observe a decrease in the oxygen basicity with decreasing metal size. O_{4b}−C bond formation is easier in the case of Cs^+ than in the presence of Li^+. Which factor dominates depends on the type of alkali cation and the type of reagent.

The harder the metal is, the stronger the M···OH or M···I interaction is, and the easier the breaking of the C−OH or C−I bond is. Therefore we can expect a decrease in the activation energy barrier with increasing alkaline metal hardness. On the other hand, the formation of the C−O_{4b} bond depends on the oxygen basicity. The larger the size of the metal, the more basic is O_{4b} (according to the MEP values) and the easier is the formation of the C−O_{4b} bond. Here the activation energy increases with increasing metal hardness. It becomes clear that the nature of the metal leads to competing effects on the methylation process through the M···OH /M···I interaction and oxygen basicity.

This is verified when comparing the energy profiles for methanol and methyl iodide. For methanol the activation energy decreases with increasing hardness of the metal. The hardness of the oxygen of the hydroxyl group is quite important and leads to a strong hard/hard interaction with the alkali cation. Therefore in the case of methanol the M···OH interaction prevails over O_{4b} basicity, as shown in the energy profiles (Figure 3). For methyl iodide, in the cluster (excluding Na^+) and in the ONIOM2 model, the activation energies decrease with increasing size of the metal. Since iodide is clearly not a hard center, the M···I interaction is relatively small, and the C−I bond is also much weaker than the C−OH bond. Thus the basicity of O_{4b} prevails over the M···I interaction. This explains the decrease in the activation energy values with increasing metal cation size for methyl iodide.

In a study by Mota and co-workers on the methylation of ZSM-5 by chloromethane, it was shown that the activation energy increases with the size of the cation. The authors concluded that the M···Cl interaction is the driving force of the reaction.[57] In the present study we show that the oxygen basicity (both related to the metal hardness) competes with the direct interaction of the metal. Moreover the oxygen basicity may prevail over the metal influence and change the order in the activation energy sequence. This depends on the hardness of the group interacting with the metal.

Both aspects have to be considered in the interpretation of experimental data. In the measurement of the NMR shielding on the chemisorbed methyl group, the cation is already bond to iodide or the hydroxyl. Thus, the only influence on the experimental NMR data is the oxygen basicity. In contrast, when measuring the stretching frequency of the N−H bond of adsorbed pyrrole, the cation−π interaction may prevail over the N−H···O hydrogen bond. Indeed it has been shown theoretically that the adsorption of pyrrole in zeolite is controlled by the interaction of the alkaline cation with pyrrole rather than by the oxygen basicity.[53] The problem is more difficult when considering the infrared measurements with adsorbed NO^+. After disproportionation of N_2O_4, NO_3^- and NO^+ are formed on the surface of the cation exchanged zeolite. The former is supposed to interact with the alkaline cation; the latter neutralizes the framework charge. One expects then that the NO^+ stretching frequency is independent of the nature of the cation. This is not the case. We are in the process of examining this reaction to resolve this ambiguity.

Conclusion

By considering the methylation reaction of a cation exchanged zeolite by methanol and methyl iodide, we tried to understand the nature and the role of zeolite basicity and to use good reactivity descriptors to evaluate it. The methylation reaction involves both the dissociation of the C−OH or C−I bond that depends on the alkaline metal hardness, and the formation of the C−O_{4b} bond, involving the oxygen framework basicity. We observed that the MEP computed around the framework oxygen reproduces its basicity well, increasing with the size of the cation. The activation energies of the methylation reactions reflect the alkali metal hardness and the oxygen basicity. For methylation with methanol the dominant factor is the interaction of the alkali metal with OH, leading to an increase of the activation energy with increasing size of the metal. For methylation with methyl iodide, the oxygen basicity is dominant and the activation energy decreases with the size of the cation. This shows that the effect of the metal and the oxygen basicity compete and lead to different trends of the activation energy with respect to the metal. The hardness of the metal and the oxygen basicity have to be included explicitly in theoretical calculations and in the interpretation of experimental data.

Acknowledgment. P.M. acknowledge a postdoctoral fellowship of the K.U. Leuven. This research project was financially supported by the G.O.A (concerted research actions) and I.A.P. V/3.

References and Notes

(1) Barthomeuf, D. *Stud. Surf. Sci. Catal.* **1991**, *65*, 157.
(2) Barthomeuf, D. *Catal. Rev.* **1996**, *38*, 521−612.
(3) Barthomeuf, D. *J. Phys. Chem. B* **2005**, *109*, 2047−2054.
(4) Corma, A. *J. Catal.* **2003**, *216*, 298−312.
(5) Davis, R. J. *J. Catal.* **2003**, *216*, 396−405.
(6) Grey, C. P.; Corbin, D. R. *J. Phys. Chem.* **1995**, *99*, 16821−16823.
(7) Hattori, H. *Chem. Rev.* **1995**, *95*, 537−558.
(8) Venuto, P. B. *Adv. Catal.* **1968**, *18*, 331.
(9) Heidler, R.; Janssens, G. O. A.; Mortier, W. J.; Schoonheydt, R. A. *J. Phys. Chem.* **1996**, *100*, 19728−19734.
(10) Barthomeuf, D. *Stud. Surf. Sci. Catal.* **1988**, *37*, 365.
(11) Barthomeuf, D. *J. Phys. Chem.* **1984**, *88*, 42−45.
(12) Huang, M.; Adnot, A.; Kaliaguine, S. *J. Am. Chem. Soc.* **1992**, *114*, 10005−10010.
(13) Xie, J.; Kaliaguine, S. *Catal. Lett.* **1994**, *29*, 281−291.
(14) Mortier, W. J. *J. Catal.* **1978**, *55*, 138−145.
(15) Huang, M. M.; Kaliaguine, S. *J. Chem. Soc., Faraday Trans.* **1992**, *88*, 751−758.
(16) Murphy, D.; Massiani, P.; Franck, R.; Barthomeuf, D. *J. Phys. Chem.* **1996**, *100*, 6731−6738.
(17) Hashimoto, S. *Tetrahedron* **2000**, *56*, 6957−6963.
(18) Huang, M.; Adnot, A.; Kaliaguine, S. *J. Am. Chem. Soc.* **1992**, *114*, 10005−10010.
(19) Marie, O.; Malicki, N.; Pommier, C.; Massiani, P.; Vos, A.; Schoonheydt, R.; Geerlings, P.; Henriques, C.; Thibault-Starzyk, F. *Chem. Commun.* **2005**, 1049−1051.
(20) Thibault-Starzyk, F.; Marie, O.; Malicki, N.; Vos, A.; Schoonheydt, R.; Geerlings, P.; Henriques, C.; Pommier, C.; Massiani, P. *Stud. Surf. Sci. Catal.* **2005**, *158*, 663−670.
(21) Vos, A. M.; Mignon, P.; Geerlings, P.; Thibault-Starzyk, F.; Schoonheydt, R. A. *Microporous Mesoporous Mater.* **2006**, *90*, 370−376.
(22) Bosacek, V. *J. Phys. Chem.* **1993**, *97*, 10732−10737.
(23) Bosacek, V.; Klik, R.; Genoni, F.; Spano, G.; Rivetti, F.; Figueras, F. *Magn. Reson. Chem.* **1999**, *37*, S135−S141.
(24) Bosacek, V.; Vratislav, S.; Dlouha, M. *Collect. Czech. Chem. Commun.* **2004**, *69*, 1537−1552.
(25) Sanderson, R. T. *J. Am. Chem. Soc.* **1983**, *105*, 2259−2261.
(26) Mortier, W. J.; Vangenechten, K.; Gasteiger, J. *J. Am. Chem. Soc.* **1985**, *107*, 829−835.
(27) Mortier, W. J. *Struct. Bond.* **1987**, *66*, 125−143.
(28) Mortier, W. J.; Ghosh, S. K.; Shankar, S. *J. Am. Chem. Soc.* **1986**, *108*, 4315−20.
(29) Vangenechten, K. A.; Mortier, W. J.; Geerlings, P. *J. Chem. Phys.* **1987**, *86*, 5063−5071.
(30) Heidler, R.; Janssens, G. O. A.; Mortier, W. J.; Schoonheydt, R. A. *Microporous Mater.* **1997**, *12*, 1−11.
(31) Deka, R. C.; Roy, R. K.; Hirao, K. *Chem. Phys. Lett.* **2000**, *332*, 576−582.
(32) Roy, R. K.; Krishnamurti, S.; Geerlings, P.; Pal, S. *J. Phys. Chem. A* **1998**, *102*, 3746−3755.
(33) Santos, J. C.; Contreras, R.; Chamorro, E.; Fuentealba, P. *J. Chem. Phys.* **2002**, *116*, 4311−4316.
(34) Nguyen, L. T.; De Proft, F.; Amat, M. C.; Van Lier, G.; Fowler, P. W.; Geerlings, P. *J. Phys. Chem. A* **2003**, *107*, 6837−6842.
(35) Geerlings, P.; De Proft, F.; Langenaeker, W. *Chem. Rev.* **2003**, *103*, 1793−873.
(36) Baur, W. H. *Am. Miner.* **1964**, *49*, 697−704.
(37) Frisch M. J., et al. *Gaussian 03*, A1; Gaussian Inc.: Pittsburgh, PA, 2003.
(38) Dunning, T. H., Jr.; Hay, P. J. *Modern Theor. Chem.* **1976**, *3*, 1−28.
(39) Zygmunt, S. A.; Mueller, R. M.; Curtiss, L. A.; Iton, L. E. *THEOCHEM* **1998**, *430*, 9−16.
(40) Kramer, G. J.; Van Santen, R. A.; Emeis, C. A.; Nowak, A. K. *Nature* **1993**, *363*, 529−531.
(41) Kramer, G. J.; Deman, A. J. M.; Vansanten, R. A. *J. Am. Chem. Soc.* **1991**, *113*, 6435−6441.
(42) Sauer, J. *Chem. Rev.* **1989**, *89*, 199−255.
(43) Rozanska, X.; van Santen, R. A.; Hutschka, F.; Hafner, J. *J. Am. Chem. Soc.* **2001**, *123*, 7655−7667.

(44) Vreven, T.; Morokuma, K. *J. Comput. Chem.* **2000**, *21*, 1419−1432.

(45) Roggero, I.; Civalleri, B.; Ugliengo, P. *Chem. Phys. Lett.* **2001**, *341*, 625−632.

(46) Geerlings, P.; Vos, A. M.; Schoonheydt, R. A. *THEOCHEM* **2006**, *762*, 69.

(47) Mignon, P.; Loverix, S.; Steyaert, J.; Geerlings, P. *Nucleic Acid Res.* **2005**, *33*, 1779−1789.

(48) Mignon, P.; Loverix, S.; Geerlings, P. *Chem. Phys. Lett.* **2005**, *401*, 40−46.

(49) Mignon, P.; Loverix, S.; De Proft, F.; Geerlings, P. *J. Phys. Chem. A* **2004**, *108*, 6038−6044.

(50) Baeten, A.; De Proft, F.; Geerlings, P. *Int. J. Quantum Chem.* **1996**, *60*, 931−939.

(51) Baeten, A.; De Proft, F.; Geerlings, P. *Chem. Phys. Let.* **1995**, *235*, 17−21.

(52) Haase, F.; Sauer, J. *J. Am. Chem. Soc.* **1995**, *117*, 3780−3789.

(53) van Bokhoven, J. A.; van der Eerden, A. M. J.; Prins, R. *J. Am. Chem. Soc.* **2004**, *126*, 4506−4507.

(54) Vos, A. M.; Nulens, K. H. L.; De Proft, F.; Schoonheydt, R. A.; Geerlings, P. *J. Phys. Chem. B* **2002**, *106*, 2026−2034.

(55) Correa, R. J.; Sousa-Aguiar, E. F.; Ramirez-Solis, A.; Zicovich-Wilson, C.; Moto, C. J. A. *J. Phys. Chem. B* **2004**, *108*, 10658−10662.

(56) Deka, R. C.; Hirao, K. *J. Mol. Catal. A*: *Chem.* **2002**, *181*, 275−282.

(57) Noronha, L. A.; Souza-Aguiar, E. F.; Mota, C. J. A. *Catal. Today* **2005**, *101*, 9−13.